Superconducting triangular islands as a platform for manipulating Majorana zero modes

Aidan Winblad[1] and Hua Chen[1,2]

[1] *Department of Physics, Colorado State University, Fort Collins, CO 80523, USA*
[2] *School of Advanced Materials Discovery, Colorado State University, Fort Collins, CO 80523, USA*

We study the possibility of obtaining robust Majorana zero modes (MZMs) at the corners of triangular superconducting islands, with the goal of finding alternative structures that can serve as building blocks for topological quantum computation. A spinless p-wave superconductor as a three point triangle, or triangular island, is consider in the presence of a vector potential field and we show it can be exactly solved to host MZMs on the corners. Additionally, for a hollow equilateral triangle subject to inhomogeneous supercurrents, from bulk-edge correspondence we find that MZMs can generally appear when two of the edges are of differing topological phase from the third edge. We also discuss the robustness of MZMs in possible experimental realizations of the triangular islands.

I. INTRODUCTION

For the past twenty years Majorana zero-modes (MZMs) in condensed matter systems have been highly sought after due to both its fault-tolerant topological protection and non-Abelian exchange statistics for quantum computating [1–5]. MZMs were originally proposed to be found in topological 2D p-wave superconducting vortices and at the ends of a topological 1D p-wave superconductor [6, 7]. A p-wave superconductor has yet to be discovered but innovative heterostructures have been proposed to make topological superconductors. Such systems make use of s-wave superconductors in proximity to various heterostructures: topological insulator [8–11] or Josephson junction with in plane magnetic field [12–15], 2D electron gas (2DEG) with Rashba spin-orbit coupling (SOC) and ferromagnet [16–20], ferromagnetic atomic spin chains [21–23], and quantum anomalous Hall insulator (QAHI) [24–26]. There have been strides in potential measurements of MZMs, most of these focus on one end of the wire [27–38] looking at zero-bias conductance peak (ZBP) curves and more recently both ends of a wire [39]. A new potential measurement may soon help confirm the identity of MZMs using a quantum dot and crossed Andreev reflections (CAR) in a Josephson junction [40].

The main proposal to achieve braiding of MZMs uses 1D wires to create large networks of T-junctions to create tetrons and hexons. It is not a simple task to develop these networks [41] and proposed quasi-1D systems in thin films [42], a cross Josephson junction [43], or scissor cuts on a QAHI [26] to get around the difficult engineering of 1D wire networks. We propose an alternative structure by using triangular superconducting islands, which can be easily produced with epitaxial growth [44].

A common thread of the previous work has been to use a magnetic field or Zeeman effect to induce a topological phase transition. Takasan 2022 spends some time building up why one can use supercurrents, should we also talk about that or just reference their paper and the 2012 supercurrent paper and let that be good enough? Instead it has been shown a supercurrent can induce a topological phase transtion in a given heterostructure [45, 46]. We show when using an inhomogeneous supercurrent on a minimal model MZMs can be exactly solved. Additionally, when using an inhomogeneous supercurrent on a quasi-1D or finite width hollow triangle island we can realize clean gap MZMs due to bulk-edge correspondence, even calculating an approximate topological phase diagram with broad topological parameter regimes.

OUTLINE: (Sec I is . . . , Sec II is . . .)

II. TRIANGULAR ISLANDS

A. 3-site problem and kitaev limit for tri.chain, solid triangle

We show one can get exact MZMs in a minimal three site triangular lattice. Let us start with the Hamiltonian of a spinless or spin-polarized p-wave superconductor of a triangular lattice

$$\mathcal{H} = \sum_{\langle j,l\rangle}(-tc_l^\dagger c_j + \Delta e^{i\theta_{l,j}} c_l^\dagger c_j^\dagger + h.c.) - \sum_j \mu c_j^\dagger c_j, \quad (1)$$

where t is the hopping amplitude, Δ is the superconducting order parameter, μ is the chemical potential, $\theta_{l,j}$ is the angle between sites l and j. Next, we apply a Peierls substitution to our creation(annihilation) operators of the form

$$c_l^\dagger c_j \to c_l^\dagger c_j \exp\left(-\frac{ie}{\hbar}\int_{r_j}^{r_l} \mathbf{A}\cdot d\mathbf{l}\right) \quad (2)$$

$$\to c_l^\dagger c_j e^{i\phi_{l,j}}.$$

Here the electron charge, e, and Planck's constant, $\hbar$, will be treated as natural numbers. One finds that t is the only term that picks up a phase, thus our modified Hamiltonian looks like

$$\mathcal{H} = \sum_{\langle j,l\rangle}(-te^{i\phi_{l,j}} c_l^\dagger c_j + \Delta e^{i\theta_{l,j}} c_l^\dagger c_j^\dagger + h.c.) - \sum_j \mu c_j^\dagger c_j. \quad (3)$$

It is difficult to come to any conclusion while in the complex fermion basis, but if we write our Hamiltonian in

a Majorana fermion basis we can get a clearer picture. Maybe a see supplementary material XX for derivation here. The Hamiltonian now takes the form

$$\begin{aligned}\mathcal{H} = &-\frac{i\mu}{4}\sum_j (a_j b_j - b_j a_j) \\ &-\frac{i}{4}\sum_{\langle j,l\rangle}[(t\sin\phi_{l.j} - \Delta\sin\theta_{l,j})a_l a_j \\ &\quad +(t\sin\phi_{l,j} + \Delta\sin\theta_{l,j})b_l b_j \\ &\quad +(t\cos\phi_{l,j} + \Delta\cos\theta_{l,j})a_l b_j \\ &\quad -(t\cos\phi_{l,j} - \Delta\cos\theta_{l,j})b_l a_j]. \end{aligned} \tag{4}$$

To clear things up, $\phi_{l,j} = -\phi_{j,l}$ since the direction of integration is reversed and the angle $\theta_{l,j} = \theta_{j,l} + \pi$, this ensures we have a Hermitian Hamiltonian.

Let us consider a three point triangular lattice, where each lattice point is a complex fermion housing two Majorana fermions. The bottom left point is a_1, b_1, bottom right is a_2, b_2, and the top point is a_3, b_3. Similar to Kitaev we will make the same assumptions $t = \Delta$ and $\mu = 0$. We are left with several combinations of trig terms, some of which we require to be zero. Notice how the bottom row is a Kitaev chain, we need only to look at how the bottom row interacts with the top point. Since our goal is to have two Majorana zero modes at the bottom corners, lets aim to have a_1 and b_2 be such modes. Anytime a_1 or b_2 appear in our equation we need its trig terms to cancel, eliminating these particles coupling from the rest of the system. Let us look at the coupling from site 1 to site 3, $\theta = \pi/3$, we notice the first and last term should be

$$(\sin\phi_{31} - \sin\pi/3)a_3 a_1 = 0, \tag{5}$$

$$(\cos\phi_{31} - \cos\pi/3)b_3 a_1 = 0. \tag{6}$$

This is true if $\phi_{31} = \pi/3$. Now let's consider the coupling of site 3 to site 2. The phase angle $\theta = -\pi/3$ and the two simplified equations involving b_2 are

$$(\sin\phi_{23} - \sin(\pi/3))b_2 b_3 = 0,$$

$$(\cos\phi_{23} - \cos(\pi/3))b_2 a_3 = 0.$$

Here we see $\phi_{23} = \pi/3$. A constant step-function vector potential one can get with the desired phase is

$$\mathbf{A} = \begin{cases} \dfrac{2\pi}{3\sqrt{3}a}\hat{\mathbf{y}} & x > 0 \\ \dfrac{-2\pi}{3\sqrt{3}a}\hat{\mathbf{y}} & x < 0. \end{cases} \tag{7}$$

We find this is still true if we extrapulate from a three point triangle to a triangular island because we need only to consider how the the corner Majorana fermions couple with their neighboring sites. When we calculated the energy spectrum for a full triangular island we found MZMs, however, they did not appear to live within a clean gap and nor did they have a broad range of vector potential strengths giving zero modes. Kitaev had noted one could still get a topological phase for $-2t < \mu < 2t$ and MZMs hosting at the interface of differing topologies. We would also like to find a range of chemical potentials that result in a topologically nontrivial phase.

III. TOPOLOGICAL PHASE DIAGRAM OF A FINITE WIDTH RIBBON

It appears Majorana fermions can behosted at the end points of a chain with finite width as with a Josephson-junction as seen in [], provided the width is much smaller than the Majorana fermion decay length. Expanding on these ideas we would like to induce a topological phase transition for an infinite triangular lattice ribbon. This will help create an argument using bulk-edge correspondence to inform how MZMs will form at the interfaces of triangular island edges, i.e. their corners.

We can start from Eq. 3 Since we are interested how a finite width ribbon along the x-axis behaves in a constant vector field we will fourier transform along the x-axis only. We pick the following transform to be

$$c^\dagger_{m,n} = \frac{1}{\sqrt{N}}\sum_k c^\dagger_{k,n} e^{i\mathbf{k}\cdot\mathbf{r}_m} \tag{8}$$

where $\mathbf{k} = k\hat{\mathbf{x}}$ and $\mathbf{r}_m = ma\hat{\mathbf{x}}$, and for convenience a will be treated as a natural number, too. This leads to the following block Hamiltonian

$$\mathcal{H}(k) = \frac{1}{2}\sum_k \Psi^\dagger_k \begin{pmatrix} \epsilon(k) & \delta(k) \\ \delta^\dagger(k) & -\epsilon(-k) \end{pmatrix} \Psi_k. \tag{9}$$

The $\epsilon(k)$ block is a tridiagonal with $\epsilon_0(k) = -2t\cos(k + \phi_1) - \mu$ along the diagonal, the upper diagonal is $\epsilon_1(k) = -t(e^{-i\phi_2} + e^{i(k-\phi_3)})$, and $\epsilon^*_1(k)$ along the lower diagonal. The $\delta(k)$ block is a tridiagonal with $\delta_0(k) = 2i\Delta\sin k$ along the diagonal, the upper diagonal is $\delta_1(k) = -\Delta(e^{i\theta_2} + e^{i(k+\theta_3)})$, and $-\delta_1(-k)$ along the lower diagonal. The size of each block is the number of rows along the y-axis in a ribbon.

To calculate the Majorana number we need to rewrite our Hamiltonian to be in skew-symmetric form. One such way is to write it in the Majorana fermion basis, the transformation matrix is of the form

$$u = \frac{1}{\sqrt{2}}\begin{pmatrix} 1 & 1 \\ -i & i \end{pmatrix} \tag{10}$$

To account for the finite number of rows in our ribbon we simply include a tensor product with an identity matrix of the same size, $U = u \otimes I_n$. We can now arrive at the skew-symmetric matrix with the following equation

$$A_{ch} = -iU\mathcal{H}_{ch}U^\dagger. \tag{11}$$

The Majorana number, $\mathcal{M}$, of a 1D chain is defined as

$$\mathcal{M} = \text{sgn}[\text{Pf}(A_{ch})], \tag{12}$$

where Pf stands for the Pfaffian of a skew-symmetric matrix. We make the claim this satisfies a finite width ribbon as well. When $\mathcal{M} = -1$, the ribbon is in a nontrivial topology and we would expect Majorana zero modes at its edges. As we sweep through a range of A for our vector potential we expect to see a gap closing, $\mathcal{M} = 1$, and our system take on a trivial topology, thus no Majorana zero modes would exist on the edge of a finite ribbon.

To illustrate the importance of bulk-edge correspondence in forming Majorana fermions we will now look at the edges of a hollow triangular island. We want to show the top edges can be in a trivial phase while the bottom remains in a nontrivial phase. In previous papers a constant vector potential was used along the chain's axis. If instead we use a constant vector potential step function centered on a chain with a 60 degree bend, equating it to a equilateral triangle, we can have an equivalent system to the chain model. One also finds that the vector potential has symmetry about the ribbon's axis, i.e. $\mathbf{A}$ pointing in the positive or negative y-axis yields the same result. Taking a hollow triangular island centered about the y-axis with the following vector potential

$$\mathbf{A} = \begin{cases} A\hat{\mathbf{y}} & x > 0 \\ -A\hat{\mathbf{y}} & x < 0 \end{cases} \tag{13}$$

we can examine each edge individually. Looking at Fig. 1 we can quickly determine each edge's vector potential with respect to its main axis.

The topological phase diagram for ribbons III and IV, with three rows, can be seen in Fig. 2a, we can see for varying μ and A, with $\mathbf{A} = A\hat{\mathbf{y}}$, where our system is topologically trivial (yellow) and nontrivial (blue). It appears when the vector potential is perpendicular to the ribbon it does not contribute to the topology of the system. Similarly, for ribbons I and II, with three rows, the topological phase diagram can be seen in Fig. 2b. Here we see the vector potential plays a vital role in transforming the topology.

We can now use bulk-edge correspondence to justify the production of Majorana fermions at the interfaces of the triangular islands edges, i.e. corners. We simulataneoulsy tune regions I and II to be in a trivial(nontrivial) topological phase and regions III and IV to be nontrivial(trivial) topological phase, respectively. To check we look at the numerical eigenenergy spectral flow and eigenstates of a triangular lattice with size $n = 100$, and width $w = 3$, and $A = [0, 2\pi]$. Fig. 3 shows strong agreement of MZMs appearing in the same vector potential range as seen in Fig. 2b's topological phase diagram. As expected we find MZMs at the bottom corners of the triangle where the differing topologies meet, as seen in Fig. 4.

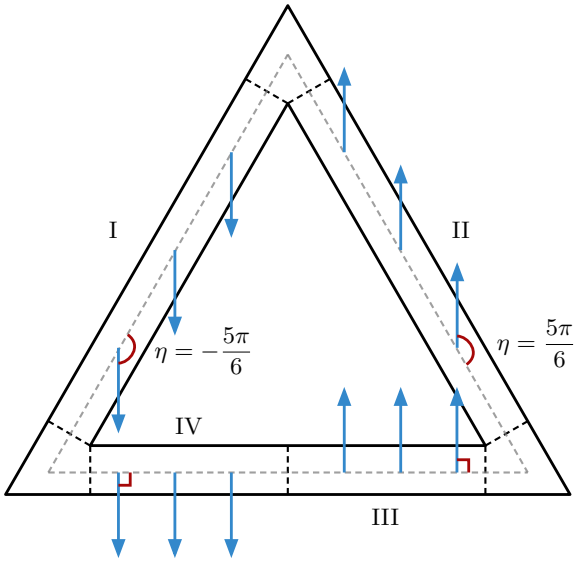

FIG. 1. Triangular island with constant step function vector potential. The edges are divided up into four regions with differing vector potentials. Each segment is treated like a finite width ribbon where we can test its topology as function of μ and $\mathbf{A}$. Vector potential $\mathbf{A}$ makes an angle $\eta = \mp\frac{5\pi}{6}, \pm\frac{\pi}{2}$, to each ribbon's main axis, respectively.

IV. CONCLUSIONS AND DISCUSSION

PLACEHOLDER

ACKNOWLEDGMENTS

Supported by XYZ Grant No. XXXXXX etc.

[1] D. A. Ivanov, Phys. Rev. Lett. **86**, 268 (2001).
[2] A. Yu. Kitaev, Annals of Physics **303**, 2 (2003).
[3] C. Nayak, S. H. Simon, A. Stern, M. Freedman, and S. Das Sarma, Rev. Mod. Phys. **80**, 1083 (2008).
[4] J. Alicea, Y. Oreg, G. Refael, F. von Oppen, and M. P. A. Fisher, Nature Phys **7**, 412 (2011).
[5] D. Aasen, M. Hell, R. V. Mishmash, A. Higginbotham, J. Danon, M. Leijnse, T. S. Jespersen, J. A. Folk, C. M. Marcus, K. Flensberg, and J. Alicea, Phys. Rev. X **6**, 031016 (2016).
[6] N. Read and D. Green, Phys. Rev. B **61**, 10267 (2000).
[7] A. Y. Kitaev, Phys.-Usp. **44**, 131 (2001).

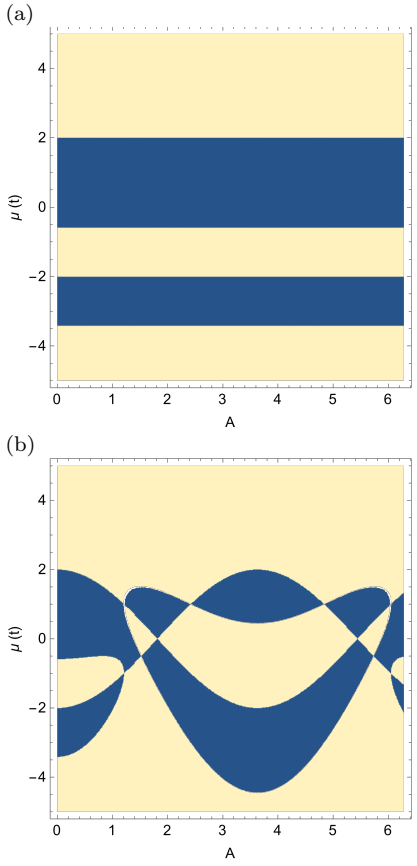

FIG. 2. Topological phase diagrams for a system with three rows (a) regions III and IV, and (b) regions I and II, from Fig. 1

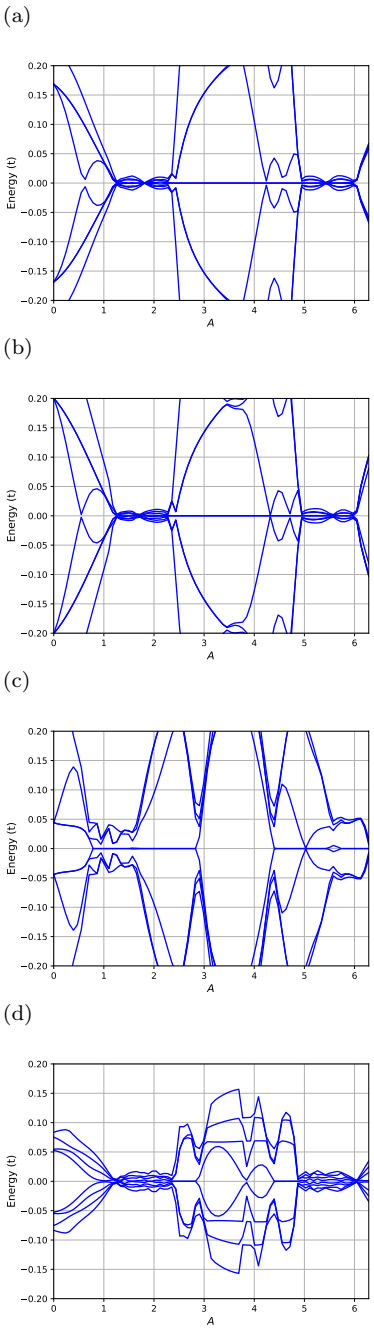

FIG. 3. Eigenenergy spectral flow for a system with $n_r = 100$ and $w_{edge} = 3$, with (a) $\mu = 0$, (b) $\mu = 0.2t$, (c) $\mu = 1.6t$, and (d) $\mu = -1.6t$.

[8] L. Fu and C. L. Kane, Phys. Rev. Lett. **100**, 096407 (2008), arxiv:0707.1692 [cond-mat].
[9] P. Hosur, P. Ghaemi, R. S. K. Mong, and A. Vishwanath, Phys. Rev. Lett. **107**, 097001 (2011).
[10] A. C. Potter and P. A. Lee, Phys. Rev. B **83**, 184520 (2011).
[11] M. Veldhorst, M. Snelder, M. Hoek, C. G. Molenaar, D. P. Leusink, A. A. Golubov, H. Hilgenkamp, and A. Brinkman, physica status solidi (RRL) – Rapid Research Letters **7**, 26 (2013).
[12] A. M. Black-Schaffer and J. Linder, Phys. Rev. B **84**, 180509 (2011).
[13] F. Pientka, A. Romito, M. Duckheim, Y. Oreg, and F. von Oppen, New J. Phys. **15**, 025001 (2013).
[14] M. Hell, M. Leijnse, and K. Flensberg, Phys. Rev. Lett. **118**, 107701 (2017).
[15] B. Scharf, F. Pientka, H. Ren, A. Yacoby, and E. M. Hankiewicz, Phys. Rev. B **99**, 214503 (2019).
[16] Y. Oreg, G. Refael, and F. von Oppen, Phys. Rev. Lett. **105**, 177002 (2010).
[17] J. D. Sau, R. M. Lutchyn, S. Tewari, and S. Das Sarma, Phys. Rev. Lett. **104**, 040502 (2010).
[18] R. M. Lutchyn, T. D. Stanescu, and S. Das Sarma, Phys. Rev. Lett. **106**, 127001 (2011).
[19] A. C. Potter and P. A. Lee, Phys. Rev. B **85**, 094516 (2012).
[20] S. Nadj-Perge, I. K. Drozdov, B. A. Bernevig, and A. Yazdani, Phys. Rev. B **88**, 020407 (2013).
[21] T.-P. Choy, J. M. Edge, A. R. Akhmerov, and C. W. J. Beenakker, Phys. Rev. B **84**, 195442 (2011).
[22] B. Braunecker and P. Simon, Phys. Rev. Lett. **111**, 147202 (2013).
[23] J. Klinovaja, P. Stano, A. Yazdani, and D. Loss, Phys. Rev. Lett. **111**, 186805 (2013).
[24] C.-Z. Chen, Y.-M. Xie, J. Liu, P. A. Lee, and K. T. Law, Phys. Rev. B **97**, 104504 (2018).

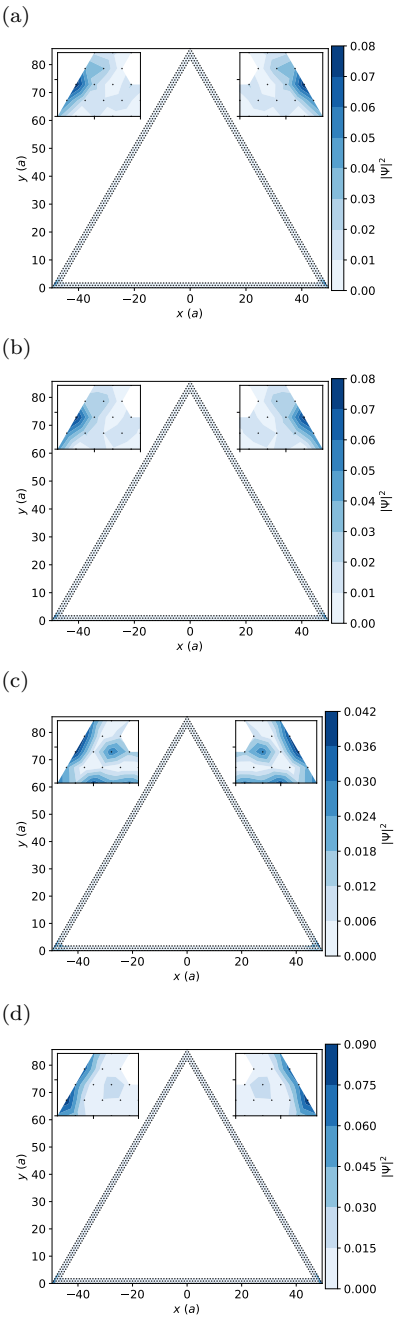

FIG. 4. MZMs for a system with $n_r = 100$ and $w_{edge} = 3$, with (a) $\mu = 0.2t$, $A = 2.8274$, (b) $\mu = 0.2t$, $A = 2.5918$, (c) $\mu = 1.6t$, $A = 2.6704$, and (d) $\mu = -1.6t$, $A = 2.4347$.

[25] Y. Zeng, C. Lei, G. Chaudhary, and A. H. MacDonald, Phys. Rev. B **97**, 081102 (2018).

[26] Y.-M. Xie, X.-J. Gao, T.-K. Ng, and K. T. Law, Creating Localized Majorana Zero Modes in Quantum Anomalous Hall Insulator/Superconductor Heterostructures with a Scissor (2021), arxiv:arXiv:2012.15523.

[27] V. Mourik, K. Zuo, S. M. Frolov, S. R. Plissard, E. P. A. M. Bakkers, and L. P. Kouwenhoven, Science **336**, 1003 (2012).

[28] L. P. Rokhinson, X. Liu, and J. K. Furdyna, Nature Phys **8**, 795 (2012).

[29] M. T. Deng, C. L. Yu, G. Y. Huang, M. Larsson, P. Caroff, and H. Q. Xu, Nano Lett. **12**, 6414 (2012).

[30] S. Nadj-Perge, I. K. Drozdov, J. Li, H. Chen, S. Jeon, J. Seo, A. H. MacDonald, B. A. Bernevig, and A. Yazdani, Science **346**, 602 (2014).

[31] J.-P. Xu, M.-X. Wang, Z. L. Liu, J.-F. Ge, X. Yang, C. Liu, Z. A. Xu, D. Guan, C. L. Gao, D. Qian, Y. Liu, Q.-H. Wang, F.-C. Zhang, Q.-K. Xue, and J.-F. Jia, Phys. Rev. Lett. **114**, 017001 (2015).

[32] S. M. Albrecht, A. P. Higginbotham, M. Madsen, F. Kuemmeth, T. S. Jespersen, J. Nygård, P. Krogstrup, and C. M. Marcus, Nature **531**, 206 (2016).

[33] H.-H. Sun, K.-W. Zhang, L.-H. Hu, C. Li, G.-Y. Wang, H.-Y. Ma, Z.-A. Xu, C.-L. Gao, D.-D. Guan, Y.-Y. Li, C. Liu, D. Qian, Y. Zhou, L. Fu, S.-C. Li, F.-C. Zhang, and J.-F. Jia, Phys. Rev. Lett. **116**, 257003 (2016).

[34] D. Wang, L. Kong, P. Fan, H. Chen, S. Zhu, W. Liu, L. Cao, Y. Sun, S. Du, J. Schneeloch, R. Zhong, G. Gu, L. Fu, H. Ding, and H.-J. Gao, Science **362**, 333 (2018).

[35] B. Jäck, Y. Xie, J. Li, S. Jeon, B. A. Bernevig, and A. Yazdani, Science **364**, 1255 (2019).

[36] A. Fornieri, A. M. Whiticar, F. Setiawan, E. Portolés, A. C. C. Drachmann, A. Keselman, S. Gronin, C. Thomas, T. Wang, R. Kallaher, G. C. Gardner, E. Berg, M. J. Manfra, A. Stern, C. M. Marcus, and F. Nichele, Nature **569**, 89 (2019).

[37] H. Ren, F. Pientka, S. Hart, A. T. Pierce, M. Kosowsky, L. Lunczer, R. Schlereth, B. Scharf, E. M. Hankiewicz, L. W. Molenkamp, B. I. Halperin, and A. Yacoby, Nature **569**, 93 (2019).

[38] S. Manna, P. Wei, Y. Xie, K. T. Law, P. A. Lee, and J. S. Moodera, Proceedings of the National Academy of Sciences **117**, 8775 (2020).

[39] L. Schneider, P. Beck, J. Neuhaus-Steinmetz, L. Rózsa, T. Posske, J. Wiebe, and R. Wiesendanger, Nat. Nanotechnol. **17**, 384 (2022).

[40] G.-H. Feng and H.-H. Zhang, Phys. Rev. B **105**, 035148 (2022).

[41] T. Karzig, C. Knapp, R. M. Lutchyn, P. Bonderson, M. B. Hastings, C. Nayak, J. Alicea, K. Flensberg, S. Plugge, Y. Oreg, C. M. Marcus, and M. H. Freedman, Phys. Rev. B **95**, 235305 (2017).

[42] A. C. Potter and P. A. Lee, Phys. Rev. Lett. **105**, 227003 (2010).

[43] T. Zhou, M. C. Dartiailh, W. Mayer, J. E. Han, A. Matos-Abiague, J. Shabani, and I. Žutić, Phys. Rev. Lett. **124**, 137001 (2020).

[44] O. Pietzsch, S. Okatov, A. Kubetzka, M. Bode, S. Heinze, A. Lichtenstein, and R. Wiesendanger, Phys. Rev. Lett. **96**, 237203 (2006).

[45] A. Romito, J. Alicea, G. Refael, and F. von Oppen, Phys. Rev. B **85**, 020502 (2012).

[46] K. Takasan, S. Sumita, and Y. Yanase, Phys. Rev. B **106**, 014508 (2022).